Asian Journal of Chemistry; Vol. 37, No. 5 (2025), 1176-1182

ASIAN JOURNAL OF CHEMISTRY

https://doi.org/10.14233/ajchem.2025.33650

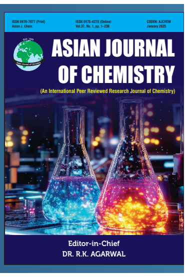

Novel Cu(II) Complexes of 3,5-Di-*tert*-butyl-2-hydroxy benzylidene-2-aminobenzhydrazide: Synthesis, Spectral Characterization, Antimicrobial and Antioxidant Properties

SANGEETA KORANE[1,*] and BABASAHEB BHOSALE[2]

[1]Department of Chemistry, Rajarshi Chhatrapati Shahu College, Kolhapur-416005, India
[2]Department of Chemistry, Rajaram College, Kolhapur-416004, India

*Corresponding author: E-mail: koranesangeeta9@gmail.com

Received: 9 March 2025; *Accepted*: 12 April 2025; *Published online*: 30 April 2025; AJC-21985

The present study reports the synthesis and characterization of three copper(II) complexes of novel hydrazone ligand 3,5-di-*tert*-butyl 2-hydroxy benzylidene 2-aminobenzhydrazide [H_2L]. The complexes *viz.* [Cu(HL)(Cl_2)H_2O] (**1a**), [Cu(HL)(NO_3)]·2/3H_2O (**2a**), [{Cu(HL)}$_2$(μ-SO_4)]·1^1/$_3$$H_2O$ (**3a**) and ligand (H_2L) were characterized by elemental analysis, spectroscopic techniques (FT-IR, ^{1}H NMR, ^{13}C NMR, UV-visible, LC-MS and PXRD), molar conductance, magnetic susceptibility measurement and thermal analysis. Thermal data of complexes at different temperatures provides the valuable information about different fragments of structure, their molecular weights, thermal stability, coordinated and fractional number of lattice water molecules in the synthesized metal complexes. Complex **1a** exhibit distorted octahedral geometry, whereas complexes **2a** and **3a** exhibit square planer to square pyramidal geometry inferred from magnetic, electronic and spectroscopic data. In all the complexes, the ligand coordinate to metal in tridentate mode through the ONO [$O_{Ketonic}$, $N_{azomethine}$ and $O_{phenolic}$] chelating system. The antibacterial potential of synthesized molecules have been determined against Gram+ve and Gram-ve bacteria *Bacillus subtilis*, *Bacillus cereus*, *Escherichia coli*, *Pseudomonas vulgaris*, *Staphylococcus aureus*, *etc*. The antioxidant activity was also determined using DPPH radical scavenging assay. It is clear that the new complexes are good active compounds for use in a variety of applications.

Keywords: Copper(II) complexes, Hydrazone, Antimicrobial activity, Antioxidant activity, Square pyramidal, Thermal studies.

INTRODUCTION

According to report of Global Research on Antimicrobial Resistance (GRAM) project, death of nearly 1.2 million people per year due to infection of drug resistant microbes [1]. Hence to develop innovative and more effective antimicrobial drugs has been the challenge for the researchers [2]. Great interest has been seen in the last decades to the chemistry of hydrazone having -CH=N-NH-linkage in its structure [3,4]. In the field of coordination chemistry they function as multidentate ligand due to presence of different heteroatoms in its structure [5]. Transition metal(II) complexes of hydrazones and hydrazides reflects multiple chelating capability and structural flexibility [6,7]. The nitrogen atom of azomethine is very instinctive as it readily interconnect with active species in biological molecule through hydrogen bonding improving their biological activities [8]. A wide range of pharmacological activities of hydrazone complexes are well known and shows influential antibacterial, anticancer, antitumour and antioxidant properties [9-13].

Among the essential elements for life, copper facilitates a wide variety of metabolic reactions including oxido-reduction, electron transport and oxygen transfer [14]. Copper complexes of hydrazone also shows extensive biological, catalytic and analytical applications [15-18]. Deng *et al.* [19] synthesized Cu(II) acetylpyridine benzoyl hydrazone complexes and shows significant anticancer and antitumour activities. Shebl *et al.* [20] evaluated the antimicrobial properties of Cu(II) complexes of hydrazone ligand derived from 4,6-diacetylresorcinol. Antimicrobial and antioxidant properties of B-formyl chromone hydrazone complexes were reported by Philip *et al.* [21]. Several reports are available on benzhydrazide derivatives too [22,23]. However no report are available on hydrazone Schiff base derived from 3,5-di-*tert*-butyl-2-hydroxy benzaldehyde and 2-amino benzhydrazide. Therefore, in view of our interest in synthesis of new Schiff base complex, we reported three novel

Cu(II) metal complexes of tridentate ONO donor aroyl-hydrazone formed by the condensation of 2-amino benzhydrazide with 3,5-di-*tert*-butyl-2-hydroxy benzaldehyde. The biological activities of the synthesized copper(II) complexes were also evaluated.

EXPERIMENTAL

All the chemicals used in the synthesis of 3,5-di-*tert*-butyl-2-hydroxy benzylidene 2-aminobenzhydrazide and copper(II) complexes were procured from Sigma-Aldrich, USA and Spectrochem, Mumbai, India. The highly pure methanol solvent was purchased from Loba Chemicals, Mumbai, India. All the reactions were carried out under normal atmospheric conditions.

Characterization: ^{1}H NMR and ^{13}C NMR spectra of Schiff base ligand in DMSO-d_6 solvent was recorded on Bruker 400.13 MHz instrument. The IR frequencies were recorded on Bruker (ALPHA) FT-IR spectrophotometer in wavelength range 4000-400 cm^{-1}. Electronic transitions in DMF solvent were recorded on Shimadzu UV-2100 Spectrophotometer. LC/MS spectra of ligands and complexes were measured on AB Sciex 3200 Q Trap model in 10% DMSO solution in isopropanol and water. TGA analysis of all the copper(II) complexes were performed with universal TA instruments, USA (SDT Q600). The CHN elemental analysis was carried out using vario EL III CHNS elemental analyzer at the SAIF Kochi, India. PXRD Study of samples were recorded on D-8 Bruker AXS diffractometer using Cu$K\alpha$ radiation ($\lambda = 1.54$ Å) Molar conductance were measured in DMF (10^{-3} M) solution using Elico conductivity bridge-180 model while the magnetic susceptibilities were observed using Gouy magnetic balance at room temperature.

Synthesis methods

Schiff base ligand (H_2L): Ligand 3,5-di-*tert*-butyl-2-hydroxy benzylidene 2-aminobenzhydrazide was synthesized by reported procedure [24]. In brief, 1 mmol of methanolic solution of 3,5-di-*tert*-butyl-2-hydroxy benzaldehyde (0.367 g) and 2-amino benzhydrazide (0.170 g) in the same solvent were refluxed together for 2 h at room temperature after adding few drops of glacial acetic acid. Separated crystals were filtered and washed with methanol, recrystallized in DMF and dehydrated in a desiccator with $CaCl_2$ (**Scheme-I**). Yield: 0.220 mg, 77.19%, Anal. calcd. (found) % for $C_{22}H_{29}N_3O_2$, calcd. (found): C, 71.90 (71.50); H, 7.95 (7.50); N, 11.43 (11.20). FT-IR (KBr, cm^{-1}): 3415 ν(O-H), 3183, 3324 ν(NH_2-sym. and asym.), 2964 ν(N-H), 1654 ν(C=O), 1610 ν(C=N), 1160 ν(N-N); LC-MS, molecular ion peak (M^+): *m/z*, 366.2; ^{1}H NMR (DMSO-d_6) δ ppm: 12.08 (1H, s, -OH), 11.60 (1H, s, -NH), 8.38 (1H, s, -CH=N), 6.029-7.67 (m, ArH), 1.22 (3H, s, *t*-butyl); ^{13}C NMR, DMSO-d_6, δ ppm: 30.55-35.02 (*t*-butyl group), 113.36-136.24 (aromatic carbon), 150.36 (-C-NH_2), 150.67 (-C-OH), 155.22 (-CH=N), 165 (-C=O); UV-visible (DMF, nm): 204, 358.

Synthesis of copper(II) complexes: The copper(II) complexes were synthesized by refluxing hot methanolic solution of ligand (1 mmol, 0.367 g) and methanolic solution of copper(II) salt *viz*. $CuSO_4·5H_2O$ (0.249 g), $CuCl_2·2H_2O$ (0.170 g) and $Cu(NO_3)_2·3H_2O$ (0.241 g), respectively using magnetic stirrer for 3 h. The resulting solids were filtered off, washed several times with methanol, recrystallized in DMF and dried in desiccator over $CaCl_2$ [25].

Antimicrobial activity: The *in vitro* antibacterial activity studies were carried out using agar well-diffusion method and the Gram-positive bacterium (pathogenic microbes) *Bacillus cerus*, *Bacillus subtilis*, *Staphylococcus aureus* and Gram-negative bacterium *Pseudomonas vulgaris*, *Escherichia coli* were selected. Ciprofloxacin is used as standard antimicrobial drug. In this method, the bacterial suspension were spread across the nutrient agar medium. The test compounds in measured quantities were dissolved in DMSO which has no inhibition activity [26]. In agar well diffusion method, wells of 0.7 cm

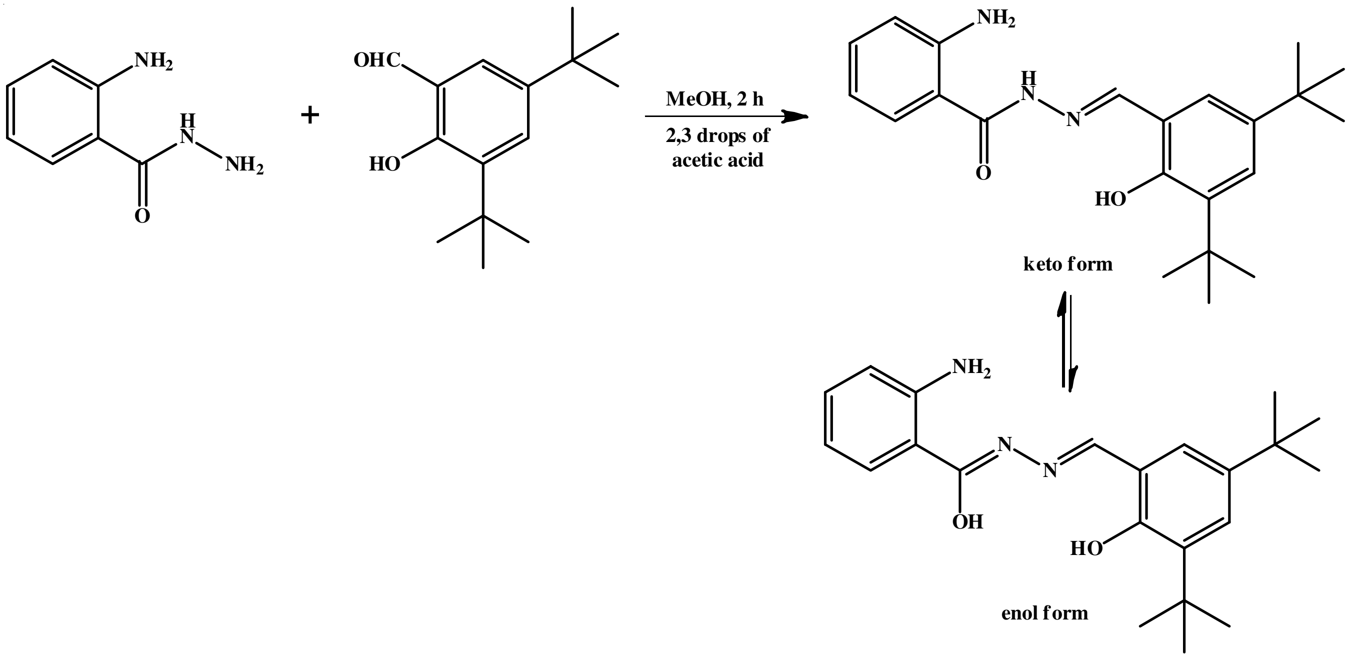

Scheme-I: Synthesis of ligand (H_2L)

diameters were formed on culture plates and loaded with the test samples (1 mg mL^{-1} in DMSO). Initially temperature of samples were 4 ºC for few hours and then incubated at 37 ºC for 24 h in incubator. Varied concentration (100, 200 and 400 µg/mL) of samples were used for diffusion and the antimicrobial potential was recorded accordingly.

Antioxidant activity: DPPH radical scavenging assay was used to measure the antioxidant potential of copper(II) complexes [27]. The free radical 2,2′-diphenyl-1-picrylhydrazyl (DPPH) was reversibly reduced the purple colour and shows the strong absorption maxima at λ 517 nm. The measurement concentration range of samples are kept from 100 to 500 µg mL^{-1}. At each time 2 mL of 1.0 mmol L^{-1} DPPH reagent in methanol was mixed with 1 mL of sample solution. Then sample under study was kept in dark for 30 min at 37 ºC for incubation. Absorbance of test samples were observed at 570 nm on spectrophotometer (UV-1800, Shimadzu, Japan). The percentage of DPPH radical scavenging activity (% RSA) was calculated using the following equation:

$$\text{RSA (\%)} = \frac{A_{\text{control}} - A_{\text{sample}}}{A_{\text{control}}} \times 100$$

where A_{control} = the absorbance of the control and A_{sample} = the absorbance of the sample.

RESULTS AND DISCUSSION

3,5-Di-*tert*-butyl-2-hydroxy benzylidene-2-amino benzhydrazide was synthesized by refluxing equimolar amount of 3,5-di-*tert*-butyl -2-hydroxy benzaldehyde with 2-amino benzhydrazide in methanol solvent for 2 h. Copper(II) complexes were synthesized by condensing Cu(II) salt and ligand solution in methanol solvent. All the Cu(II) complexes are stable, coloured, high melting point and insoluble in common organic solvents like methanol, ethanol, benzene, carbon tetrachloride *etc.* but soluble in DMSO and DMF solvents. The physico-analytical data of the ligand and its copper complexes are given in Table-1. The molar conductance values of copper(II) complexes in DMF (10^{-3} M) are very less (Table-1) indicating its non-electrolytic in nature [28,29].

FTIR studies: The FT-IR spectral data for ligand (H_2L) and its Cu(II) complexes are shown in Table-2. The FT-IR spectra of ligand shows ν(-OH) transition at 3415 cm^{-1} become invisible in all the complexes suggesting coordination of phenolic -OH group to metal center. It is further strengthened by upward shifting of ν(C-O) phenolic frequency from 1282 cm^{-1} in ligand to 1315-1309 cm^{-1} in complexes [30]. The ν(C=N) stretching frequency is specified in the range 1610 cm^{-1} for H_2L indicates condensation of hydrazide with aldehyde. In complexes **1a**, **2a**, **3a**, appearance of new peak at 1605-1530 cm^{-1} region suggesting coordination of azomethine nitrogen to metal [31]. It is supported by shifting of N-N stretching frequency to higher wavenumber from 1160 cm^{-1} in ligand to 1165-1166 cm^{-1} in the complexes [30]. In IR spectra of H_2L, ν(C=O) stretching vibrations are observed at 1654 cm^{-1} suggesting the amido form in the solid state of hydrazones. The medium ν(N-H) stretching vibrations of NH group at 2964 cm^{-1} supports above statement. In complexes, the ν(N-H) stretching vibrations are also observed from 2953-2952 cm^{-1} and ν(C=O) vibrational frequency are observed at 1644-1604 cm^{-1} in copper complexes suggesting the coordination of oxygen of ketonic group to metal center [30,32,33]. Two bands at 3324 cm^{-1} and 3183 cm^{-1} are due to the symmetric and asymmetric stretching vibrations of NH_2 group [34]. The spectra of complex **2a** reflect band at 1375 for ν(N-O) vibrations [35], wehreas in copper complexes, the medium stretching bands at 596-504 cm^{-1} and 692-659 cm^{-1} are due to Cu-N and Cu-O vibrations [36]. Thus in all the three copper(II) complexes, Schiff base ligand is coordinated to the metal through phenolic oxygen, azomethine nitrogen and oxygen of ketonic group.

NMR studies: A sharp singlet at 12.098 ppm in downfield region in ^1H NMR spectrum H_2L is due to hydroxyl protons (phenolic-OH group). The hydrazide protons (-N-H) in the hydrazones shows singlet at 11.60 ppm [37] suggest the ketonic nature of ligand in solution. The singlet peaks are recorded for both protons indicates the coupling interactions of protons on neighbouring atoms are not possible. The azomethine protons resonate at 8.38 ppm and the multiplets observed at 6.50 to 7.96 ppm range are due to aromatic protons [38]. The protons

TABLE-1
PHYSICO-ANALYTICAL DATA OF LIGAND AND ITS COPPER(II) COMPLEXES

Compd.	m.f.	m.w.	Colour	Yield (%)	m.p. (ºC)	Elemental analysis (%): Calcd. (found)				Molar cond. (ohm^{-1} cm^2 mol^{-1})
						C	H	N	M	
H_2L	$C_{22}H_{29}N_3O_2$	367.48	White	77.19	250	71.50 (71.90)	7.50 (7.95)	11.20 (11.43)	–	–
1a	$C_{22}H_{30}N_3O_3CuCl_2$	520.93	Green	70.87	>300	50.25 (50.67)	6.01 (5.80)	8.30 (8.06)	12.50 (12.27)	15.30
2a	$C_{22}H_{30}N_4O_6Cu$	504.48	Green	71.17	>300	51.90 (52.38)	5.45 (5.99)	11.48 (11.10)	12.20 (12.68)	8.70
3a	$C_{44}H_{58}N_6O_9Cu_2S$	979.9	Green	73.29	>300	54.10 (53.87)	6.15 (5.95)	8.90 (8.56)	13.18 (13.04)	10.45

TABLE-2
FT-IR SPECTRAL DATA (cm^{-1}) OF LIGAND AND ITS COPPER(II) COMPLEXES

Compound	ν(-OH)	ν(N-H)	ν(C=N)	ν(C=O)	ν(C-O)/ (phenolic)	ν(N-N)	ν(M-N)	ν(M-O)
H_2L	3415	2964	1610	1654	1282	1160	–	–
$[Cu(HL)(Cl_2)\ H_2O]$ (**1a**)	–	2952	1562	1614	1309	1166	692	659
$[Cu(HL)(NO_3)]\cdot 2/3H_2O$ (**2a**)	–	2953	1605	1644	1315	1165	660	596
$[\{Cu(HL)\}_2(\mu\text{-}SO_4)]\cdot 1^1/_3H_2O$ (**3a**)	–	2952	1530	1604	1313	1165	659	504

of amino group shows singlet at 6.029 ppm. The *tert*-butyl group in H_2L reflect the chemical shift in 1.20-1.35 ppm range.

In ^{13}C NMR spectra of ligand, the carbonyl carbon and azomethine carbon shows the chemical shift at 165.42 ppm and 155.22 ppm, respectively. The phenolic (C-OH) and amino (C-NH_2) groups reflect the chemical shift at 150.67 ppm and 150.36 ppm. The carbons in aromatic region resonate from 113.36-136.24 ppm [38-40]. The *tert*-butyl group of H_2L reflect chemical shift at 30.55-35.02 ppm. ^{1}H NMR and ^{13}C NMR spectra of copper(II) complexes are not obtained due to its paramagnetic nature and less solubility in DMSO solution [30].

Mass spectral studies: The mass spectra of Schiff base ligand is shown by Fig. 1. The molecular ion peak as well as base peak appeared at 367.4 amu for H_2L corresponding to ligand moiety ($C_{22}H_{29}N_3O_2$, atomic mass $m/z = 367.48$). Some stable fragments observed are 66.0 $[C_5H_6 + H]^+$, 80.0 $[C_6H_6 + 2H]^+$, 94.9 $[C_6H_8N]^+$, 135.0 $[C_7H_7N_2O\text{-}2H]^+$ and 230.4 $[C_{15}H_{22}NO\text{-}2H]^+$. *etc.*

TABLE-3
ELECTRONIC SPECTRAL DATA OF COMPLEXES

Compound	$\mu_{effective}$ (B.M.)	Absorption maxima (cm^{-1})	Spectral assignments
H_2L		490196	n-π*
		279329	π-π*
1a	1.74	416666	n-π*
		344827	π-π*
		246913	LMCT
		120481	*d-d* transition
2a	1.71	444444	n-π*
		338983	π-π*
		240963	LMCT
		161290	*d-d* transition
3a	1.55	444444	n-π*
		344827	π-π*
		239234	LMCT
		156250	*d-d* transition

Electronic spectral and magnetic susceptibility studies: The UV-visible spectral assignments of complexes in DMF solvent were recorded and the results are shown in Table-3. This technique is helpful to other methods of characterization to evaluate the structure of complex. The intra-ligand transitions n-π* and π-π* of azomethine group and aromatic ring are observed in hydrazones at 204-358 nm and in metal complexes, these transition are shifted and shows absorption at 225-295 nm due to the linkage of azomethine nitrogen to metal. Copper(II) complexes (**1a**, **2a** and **3a**) show the sharp and broad LMCT bands at 246913, 240963 and 239234 cm^{-1}, which are due to the combination of charge transfer transitions from 'O' and 'N' donor atom of ligand to metal centre [33]. A broad *d-d* band observed at 120481 cm^{-1} for complex **1a** is due to ligand field and Jahn-Teller effect assign $^2E_g \rightarrow {}^2T_{2g}$ transition shows the tetragonal distortion observed in octahedral geometry, the width of band supports evidence for distortion. The octahedral distortion is evident in the magnetic moment of 1.74 B.M., which is greater than the predicted value of 1.73 B.M., for a single unpaired electron [8,30]. The Cu(II) in d^9 orbital has d^2

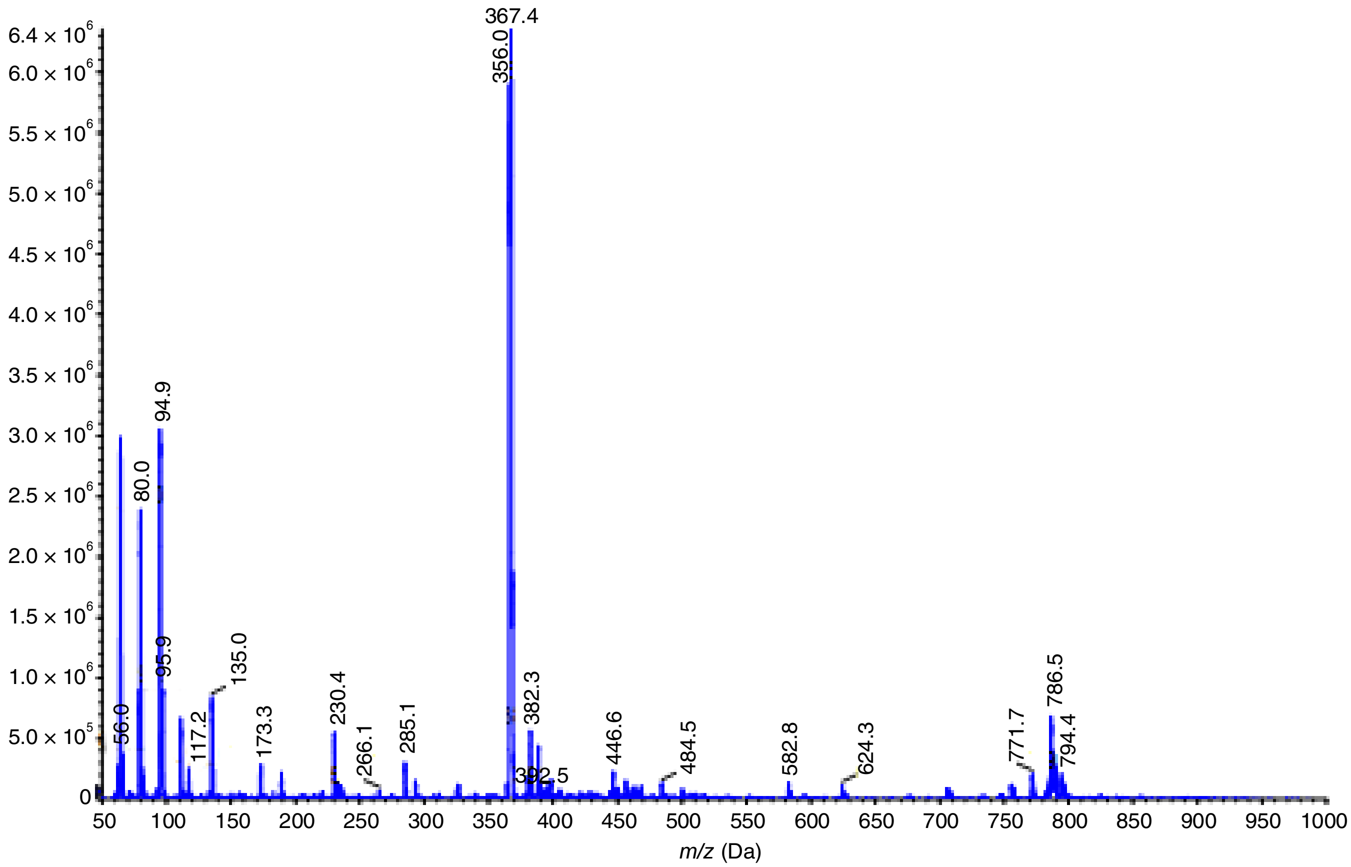

Fig. 1. Mass spectrum of ligand H_2L

ground term and in lower symmetry, square planar complexes has $dx^2–y^2$ ground state. Three transitions ($dx^2–y^2 \rightarrow dxy$, $dx^2–y^2 \rightarrow dz^2$, $dx^2–y^2 \rightarrow dxz, dyz$ ($^2B_{2g} \leftarrow {}^2B_{1g}$, $^2A_{1g} \leftarrow {}^2B_{1g}$, $^2E_g \leftarrow {}^2B_{1g}$) are expected, however, due to the close proximity of *d*-levels, the four orbitals have almost the same energy, making it difficult to assign these bands indep-endently. Hence, the broad *d-d* bands observed in spectra at 161290 for complex **2a** and 156250 cm^{-1} for **3a** are assigned to square planer and square pyramidal geometry, respectively [29,33]. The mag-netic moment 1.71 B.M. shown by complex **2a** support square planer [41] and 1.55 B.M. for complex **3a** suggest some Cu-Cu interactions with square pyramidal geometry [35].

XRD study: The development of single crystals of the Schiff base ligand and its three copper(II) complexes was unsuccessful after multiple efforts; therefore, the crystalline characteristics of the ligand (H_2L) and the Cu(II) complexes (**1a**, **2a** and **3a**) were assessed using PXRD analysis. The X-ray diffractogram of hydrazone ligand were scanned in the range 0-60° at wavelength 1.54 Å. The average particle size calculated from Scherrer's formula applying XRD line broadening method [2,31].

$$D = \frac{K\lambda}{\beta \cos\theta}$$

The crystallite size for H_2L was found to be 140.82 nm, which confirmed its crystalline nature. The crystallite size for copper(II) complex **1a**, **2a**, **3a** is 17.34, 31.34 and 35.43 nm, respectively suggest their crystalline nature.

Thermal studies: The thermal analysis is performed at temperature 25-780 ºC in a nitrogen atmosphere. TGA curves of complexes are shown by Fig. 2, while thermogravimetric data is given in Table-4. The TG curve of complex **1a** shows first stage decomposition at 9.17% (calcd. 10.28%) in the temperature range of 150-221 ºC indicating loss of coordinated H_2O and chlorine molecules [30]. The second weight loss of 36.88% (calcd. 36.21%) from temperature range of 225-374 ºC due to loss of organic part of ligand ($-C_{14}H_{20}$). Further weight loss of 7.21% (calcd. 6.81%) in between 374 to 433 ºC due to the loss of second chlorine molecule. Third weight loss observed at 19.91% (calcd. 19.06%) in the temperature range of 433-673 ºC happened due to the loss of organic moiety ($-C_4H_7N_2O$). Remaining organic moiety 3.42% (calcd. 5.19%) decompose

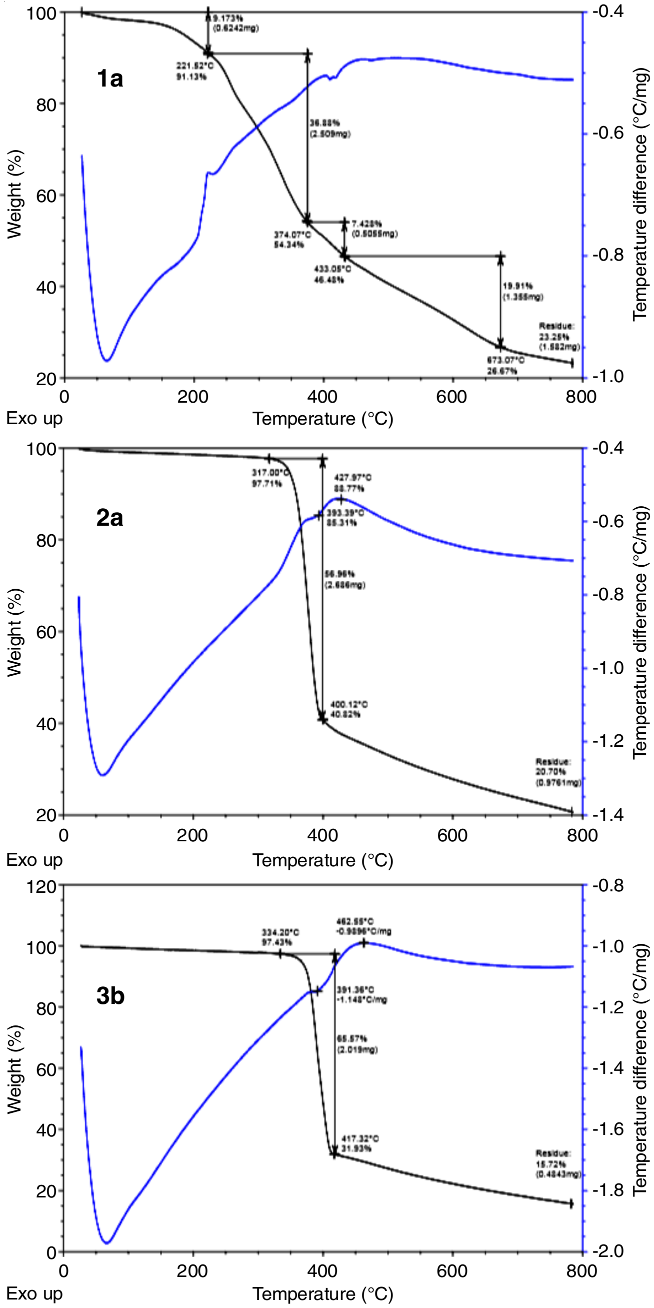

Fig. 2. Thermogravimetric curves of complex **1a**, **2a** and **3a**

TABLE-4
THERMO GRAVIMETRIC DATA OF COPPER-II COMPLEXES

Compound	Temperature range (ºC)	Mass loss (%)		Decomposition assignments
		Exp.	Calcd.	
1a	70-221	9.17	10.28	Coordinated water molecule and coordinated chloro group
	221-374	36.88	36.21	Organic moiety of aldehyde portion ($C_{14}H_{20}$)
	374-433	7.42	6.81	Coordinated chloro group
	433-700	19.91	19.06	Organic moiety ($-C_4H_7N_2O$)
	700-780	3.42	5.19	Remaining organic moiety (CHN)
	780	23.25	22.22	Residue of CuO + 3C
2a	25-85	2.29	2.37	Lattice water molecule ($-2/3H_2O$)
	317-770	77.08	79.47	Organic moiety ($-C_{21}H_{28}N_3$) and nitrate ion
	770	20.70	18.14	Metal oxide residue CuO + C
3a	25-110	2.57	2.44	Lattice water molecule ($-1^1/_3H_2O$)
	334-780	81.78	82.96	Organic moiety ($-C_{44}H_{56}N_6O_3$) and sulphate ion
	780	15.72	14.60	Metal oxide residue CuO + Cu

continuously after that temperature and finally metal oxide (CuO) and some traces of carbon 23.25% (22.22%) were obtained as residue at 780 ºC [31]. Complex **2a** shows first weight loss 2.29 % (calcd. 2.37 %) from 25 to 120 ºC suggesting the presence of 2/3 lattice water molecules. In second stage of decomposition, complex **2a** lose 77.07% (calcd. 79.47%) mainly due to the rapid loss of organic moiety in temperature range 317-400 ºC and then slowly in between 400-780 ºC due to remaining organic portion of ligand and nitrate ion. At the end, the metal oxide residue 20.70% (calcd. 18.14%) was obtained in the form of CuO and trace of carbon. In complex **3a**, the first weight loss of 2.57% (calcd. 2.44%) was observed due to the fractional number ($1^{1}/_{3}$ H_2O) of lattice water molecule. The second stage of decomposition starts at 337 ºC and ends at 780 ºC losing 81.78% (calcd. 82.96%) of organic moiety and sulphate ion initially rapidly up to 417 ºC and then slowly up to 780 ºC. Finally, the metal oxide residue 15.72% (calcd. 14.60%) was obtained at 780 ºC in the form of CuO with trace of copper metal. In all the three copper(II) hydrazone complexes weight loss of organic moiety till 780 ºC indicating strong bonding between metal and ligand.

Biological activity

Antimicrobial activity: The antimicrobial activity of synthesized hydrazone and its ccopper(II) complexes were evaluated using agar well diffusion method and the results are shown in Table-5. The zone of inhibition was calculated in mm for each microbe species. The antibacterial activity of Cu(II) complexes shows higher inhibitory zone for Gram-positive bacteria *B. cereus* since Gram-positive bacteria have more antigenic properties due to outer lipid membrane of polysaccharides [42]. During the antimicrobial action, azomethine nitrogen of hydrazone complexes forms hydrogen bond with microbes or ribosomes of microbial cells altering its normal cell processes [8]. The copper(II) complexes of hydrazone shows higher antibacterial activity than free ligand since complexes shows more lipophilic character [42]. According to concept of chelation, polarity of metal ion get decreased during complex formation due to partial sharing of positive charge with tridentate ligand. It favours the lipid solubility and permission in to normal cell of bacterial membrane [8,43]. Along with this nature of metal ion, the geometry of complex, steric and pharmacokinetic factors also play key role in improving antibacterial activity of the metal complexes [8].

Antioxidant activity: The measurement of free radical scavenging capacity requires the removal of DPPH ions with hydrogen-donating molecules and the generation of non-radicals DPPH-H in the reaction solution. Colour intensity of the DPPH solution get changed from dark to light in response to the decrease in absorbance of the test sample demonstrated that the compound has antioxidant potential [44]. In this experiment, at 100 µg, the DPPH scavenging activity of complex **1a** (8.55 ± 3.2%), **2a** (10 ± 1%) and **3a** (12.6 ± 2.5%), respectively. While scavenging activity at higher concentration of 500 µg, of complex **1a** (68 ± 2.51%), for **2a** (76 ± 4.5 %) and for **3a** (80 ± 4.16 %) percent, respectively as illustrated in Table-6.

Conclusion

The synthesis of novel hydrazone ligand 3,5-di-*tert*-butyl 2-hydroxy benzylidene 2-aminobenzhydrazide [H_2L] and its three copper(II) complexes $[Cu(HL)(Cl_2)H_2O]$ (**1a**), $[Cu(HL)(NO_3)]\cdot 2/3H_2O$ (**2a**), $[\{Cu(HL)\}_2(\mu\text{-}SO_4)]\cdot 1^{1}/_{3}H_2O$ (**3a**) were successfully accomplished. The Schiff base hydrazone ligand and its complexes were characterized by FT-IR, UV-visible, ^{1}H and ^{13}C NMR, TGA, powder XRD, magnetic susceptibility, molar conductance and elemental analysis. Based from the results of FT-IR, electronic spectra and magnetic moment, complex **1a** have distorted octahedral geometry while complexes **2a** and **3a** have square planar and square pyramidal geometry, respectively. In these complexes, the ligand behaves as monobasic tridentate, coordinate to metal center through phenolate oxygen, azomethine nitrogen and oxygen of ketonic group. All the three copper(II) complexes shows significant antibacterial and antioxidant activities.

ACKNOWLEDGEMENTS

The authors acknowledge to The NMR facility (Instrumentation Center) at Punyashlok Ahilyadevi Holkar University,

TABLE-5
ZONE OF INHIBITION (mm) OF GROWTH OF MICROORGANISMS

Compound	Minimum inhibitory concentration (µg/mL)				
	Gram-positive bacteria			Gram-negative bacteria	
	B. subtilties	*B. cereus*	*S. aureus*	*P. velgaris*	*E. coli*
H_2L	12 ± 0.70	14 ± 0.21	11 ± 0.32	10 ± 0.91	10 ± 0.35
1a	16 ± 0.10	19 ± 0.90	14 ± 0.50	15 ± 0.53	15 ± 0.53
2a	17 ± 0.51	20 ± 0.12	15 ± 0.57	16 ± 0.90	15 ± 0.70
3a	15 ± 0.57	18 ± 0.21	14 ± 0.70	14 ± 0.80	14 ± 1.00
Ciprofloxacin	21 ± 0.10	22 ± 0.80	20 ± 0.75	21 ± 0.32	20 ± 0.56

TABLE-6
ANTIOXIDANT POTENTIAL OF SYNTHESIZED MOLECULES WERE INVESTIGATED USING DPPH RADICAL SCAVENGING ASSAY

Synthesized hydrazone complexes	Concentration (µg)				
	100	200	300	400	500
1a	8.55 ± 3.2%	14.88 ± 3.2%	34.52 ± 3.3%	49.21 ± 1.2%	68 ± 2.51%
2a	10.0 ± 1.0%	18.34 ± 2.1%	39.48 ± 1.6%	57.07 ± 3.2%	76 ± 4.5 %
3a	12.66 ± 2.%	21.42 ± 1.1%	42.53 ± 2.4%	60.10 ± 2.4%	80 ± 4.16%

Solapur, India for conducting the spectral analysis. Thanks are also due the Central Facility Centre (CFC) of Shivaji University, Kolhapur, India for prodiving the facility of PXRD technique.

CONFLICT OF INTEREST

The authors declare that there is no conflict of interests regarding the publication of this article.

REFERENCES

1. S. Kariuki, *The Lancet*, **404**, 1172 (2024); https://doi.org/10.1016/S0140-6736(24)01885-3
2. N. Kumar, A. Asija, Y. Deswal, S. Saroya and A. Kumar, *Res. Chem. Intermed.*, **48**, 5133 (2022); https://doi.org/10.1007/s11164-022-04860-0
3. L. Popiolek, *Med. Chem. Res.*, **26**, 287 (2017); https://doi.org/10.1007/s00044-016-1756-y
4. J.O.C. Brum, T.C.C. França, S.R. LaPlante and J.D.F. Villar, *Mini-Rev. Med. Chem.*, **20**, 342 (2020); https://doi.org/10.2174/1389557519666191014142448
5. J. Devi, B. Kumar and B. Taxak, *Inorg. Chem. Commun.*, **139**, 109208 (2022); https://doi.org/10.1016/j.inoche.2022.109208
6. C. Anitha, C.D. Sheela, P. Tharmaraj and S. Sumathi, *Spectrochim. Acta A Mol. Biomol. Spectrosc.*, **96**, 493 (2012); https://doi.org/10.1016/j.saa.2012.05.053
7. N. Ribeiro and I. Correia, *Front. Chem. Biol.*, **3**, 1398873 (2024); https://doi.org/10.3389/fchbi.2024.1398873
8. R.S. Bhaskar, C.A. Ladole, N.G. Salunkhe, J.M. Barabde and A.S. Aswar, *Arab. J. Chem.*, **13**, 6559 (2020); https://doi.org/10.1016/j.arabjc.2020.06.012
9. A.R. Aguirre and H. Beraldo, *Polyhedron*, **256**, 116993 (2024); https://doi.org/10.1016/j.poly.2024.116993
10. S. Omidi and A. Kakanejadifard, *RSC Adv.*, **10**, 30186 (2020); https://doi.org/10.1039/D0RA05720G
11. Q.Y. Mo, J.G. Deng, Y. Liu, G.D. Huang, Z.W. Li, P. Yu, Y. Gou and F. Yang, *Eur. J. Med. Chem.*, **156**, 368 (2018); https://doi.org/10.1016/j.ejmech.2018.07.022
12. M. Chen, X. Chen, G. Huang, Y. Gou and J. Deng, *J. Mol. Struct.*, **1268**, 133730 (2022); https://doi.org/10.1016/j.molstruc.2022.133730
13. H.Q. Chang, L. Jia, J. Xu, W.N. Wu, T.-F. Zhu, R.-H. Chen, T.-L. Ma, Y. Wang and Z.-Q. Xu, *Transition Met. Chem.*, **40**, 485 (2015); https://doi.org/10.1007/s11243-015-9938-x
14. P.H.O. Santiago, M.B. Santiago, C.H.G. Martins and C.C. Gatto, *Inorg. Chim. Acta*, **508**, 119632 (2020); https://doi.org/10.1016/j.ica.2020.119632
15. M. Shakdofa, M. Shtaiwi, M. Nagy and T.M.A. Abdel-Rassel, *Main Group Chem.*, **13**,187. (2014); https://doi.org/10.3233/MGC-140133
16. I.S. Turomsha, M.Y. Gvozdev, N.V. Loginova, G.A. Ksendzova and N.P. Osipovich, *Chem. Proc.*, **12**, 73 (2022); https://doi.org/10.3390/ecsoc-26-13576
17. R. Fekri, A. Abdolmaleki, A. Asadi, A. Karimian, L. Taghizadehmomen, M. Salehi, R.K. Raheem and L. Karimian, *Basic Clin. Cancer Res.*, **13**, 143 (2021); https://doi.org/10.18502/bccr.v13i2.10029
18. K. Srishti, O. Negi and P.K. Hota, *J. Fluoresc.*, **35**, 1273 (2025); https://doi.org/10.1007/s10895-024-03587-y
19. J.G. Deng, Y. Gou, W. Chen, X. Fu and H. Deng, *Bioorg. Med. Chem.*, **24**, 2190 (2016); https://doi.org/10.1016/j.bmc.2016.03.033
20. M. Shebl, M.A. El-Ghamry, S.M.E. Khalil and M.A.A. Kishk, *Spectrochim. Acta A Mol. Biomol. Spectrosc.*, **126**, 232 (2014); https://doi.org/10.1016/j.saa.2014.02.014
21. J.E. Philip, S.A. Antony, S.J. Eeettinilkunnathil, M.R.P. Kurup and M.P. Velayudhan, *Inorg. Chim. Acta*, **469**, 87 (2018); https://doi.org/10.1016/j.ica.2017.09.006
22. B. Kumar, J. Devi, P. Saini, D. Khurana, K. Singh and Y. Singh, *Res. Chem. Intermed.*, **50**, 3915 (2024); https://doi.org/10.1007/s11164-024-05328-z
23. A. Ansari, S. Tauro and S. Asirvatham, *Mini-Rev. Org. Chem.*, **19**, 522 (2022); https://doi.org/10.2174/1570193X18666210920141351
24. F. Rahim, H. Ullah, M. Taha, A. Wadood, M.T. Javed, W. Rehman, M. Nawaz, M. Ashraf, M. Ali, M. Sajid, F. Ali, M.N. Khan and K.M. Khan, *Bioorg. Chem.*, **68**, 30 (2016); https://doi.org/10.1016/j.bioorg.2016.07.005
25. L. Balapoor, R. Bikas and M. Dargahi, *Inorg. Chim. Acta*, **510**, 119734 (2020); https://doi.org/10.1016/j.ica.2020.119734
26. P. Cos, A.J. Vlietinck, D.V. Berghe and L. Maes, *J. Ethnopharmacol.*, **106**, 290 (2006); https://doi.org/10.1016/j.jep.2006.04.003
27. C. Aware, R. Patil, S. Gaikwad, S. Yadav, V. Bapat and J. Jadhav, *Asian Pac. J. Trop. Biomed.*, **7**, 1097 (2017); https://doi.org/10.1016/j.apjtb.2017.10.012
28. G. Dongare and A.A. Aswar, *Res. Chem. Intermed.*, **50**, 745 (2024); https://doi.org/10.1007/s11164-023-05169-2
29. M. Sutradhar, E.C.B.A. Alegria, M.F.C.G. da Silva, L.M. Martins and A. Pombeiro, *Molecules*, **21**, 425 (2016); https://doi.org/10.3390/molecules21040425
30. G. Dongare and A. Aswar, *J. Saudi Chem. Soc.*, **25**, 101325 (2021); https://doi.org/10.1016/j.jscs.2021.101325
31. S.A. Aly and S.K. Fathalla, *Arab. J. Chem.*, **13**, 3735 (2020); https://doi.org/10.1016/j.arabjc.2019.12.003
32. P.E. Hansen, M. Vakili, F.S. Kamounah and J. Spanget-Larsen, *Molecules*, **26**, 7651 (2021); https://doi.org/10.3390/molecules26247651
33. A.K. Patel, R.N. Jadeja, N. Patel, R.N. Patel, S.K. Patel, R.J. Butcher, S. Kumar and G. Kumar, *Results Chem.*, **4**, 100244 (2022); https://doi.org/10.1016/j.rechem.2021.100244
34. E.E. Sengul, T. Gokturk, C.G. Topkaya and R. Gap, *J. Chil. Chem.*, **65**, 4754 (2020).
35. S.H. Seleem, G.A. El-Inany, B.A. EI-Shetary and M.A. Mousa, *Chem. Cent. J.*, **11**, 2 (2011); https://doi.org/10.1186/1752-153X-5-2
36. A.A. Alzharani, *J. Umm Al-Qura Univ. Appl. Sci.*, **9**, 455 (2023); https://doi.org/10.1007/s43994-023-00054-5
37. H. Kargar, M. Fallah-Mehrjardi, R. Behjatmanesh-Ardakani, K.S. Munawar, M. Ashfaq and M.N. Tahir, *Transition Met. Chem.*, **46**, 437 (2021); https://doi.org/10.1007/s11243-021-00460-w
38. O. Pouralimardan, A. Chamayou, C. Janiak and H. Hosseini-Monfared, *Inorg. Chim. Acta*, **360**, 1599 (2007); https://doi.org/10.1016/j.ica.2006.08.056
39. B. Shaabani, A.A. Khandar, H. Mobaiyen, N. Ramazani, S.S. Balula and L. Cunha-Silva, *Polyhedron*, **80**, 166 (2014); https://doi.org/10.1016/j.poly.2014.03.033
40. S.H. Guzar and J.I.N. Qin-Han, *J. Appl. Sci.*, **8**, 2480 (2008); https://doi.org/10.3923/jas.2008.2480.2485
41. A.A. El-Sherif, *Inorg. Chim. Acta*, **362**, 4991 (2009); https://doi.org/10.1016/j.ica.2009.08.004
42. K.Y. Djoko, M.M. Goytia, P.S. Donnelly, M.A. Schembri, W.M. Shafer and A.G. McEwan, *Antimicrob. Agents Chemother.*, **59**, 6444 (2015); https://doi.org/10.1128/aac.01289-15
43. H. Agarwal, S. Menon and V.K. Shanmugam, *Surf. Interfaces*, **19**, 100521 (2020); https://doi.org/10.1016/j.surfin.2020.100521
44. E. Koksal, E. Bursal, E. Dikici, F. Tozoglu and I. Gulcin, *J. Med. Plants Res.*, **5**, 217 (2011).